Journal of Molecular Modeling (2021) 27: 272
https://doi.org/10.1007/s00894-021-04894-y

ORIGINAL PAPER

Interaction of glyphosate in matrices of cellulose and diethylaminoethyl cellulose biopolymers: theoretical viewpoint of the adsorption process

Sílvio Quintino de Aguiar Filho[1] · Adão Marcos Ferreira Costa[1,2] · Anna Karla dos Santos Pereira[3] · Grasiele Soares Cavallini[1] · Douglas Henrique Pereira[1]

Received: 13 June 2021 / Accepted: 25 August 2021 / Published online: 1 September 2021

Abstract

Glyphosate is an herbicide widely used in agricultural activities causing contamination of soils and bodies of water and damage to the biodiversity of ecosystems. In this context, the present study aimed to theoretically study the adsorption potential of the biopolymer cellulose (CE) and its diethylaminoethyl cellulose derivative (DEAEC) with the herbicide glyphosate (GLY). Theoretical calculations were performed using the density functional theory. Molecular electrostatic potential and frontier molecular orbital analyses were performed, which allowed identifying the possible sites of interaction of biopolymers that were in the functional groups –OH and O^- of cellulose and in the groups $–O^-$ and $–NH^+(CH_2CH_3)_2$ of the DEAEC. Reactivity indices chemical softness and hardness showed that both adsorbents could interact with adsorbate. Simulated IR indicated that the interactions could be evinced in experimental measurements by changes in the bands of glyphosate (ν(P=O), δ(P-O–H), δ(C-N–H)) or in the bands of CE and DEAEC (ν(C–O), ν(C–H), ν(N–H)). The binding energies showed that the GLY interacts more effectively with CE than DEAEC. The ΔH prove that all processes are exothermic and the CE-GLY[1] interaction showed value of $\Delta G < 0$. The topological results showed a greater number of interactions with electrostatic nature. The results found in the study show that the theoretical data provides useful information to support the use of biopolymers as matrices for glyphosate adsorption or other contaminants.

Keywords Herbicide · Biopolymers · Simulations · DFT

Introduction

Resistance to herbicides by weeds has resulted in an increase in the concentration used of these pesticides [1]. The world estimate of losses in agricultural production by weeds is 34% higher than the estimated losses with animal pests and pathogens (18 and 16%) [2], making the use of pesticides necessary from an economic and agricultural point of view.

In order to reduce the environmental impacts of agricultural activities, environmental legislation for the use of pesticides and herbicides is becoming increasingly stringent [3–5]. The excessive use of herbicides has been related to the contamination of water bodies and soils, promoting an accumulation of these persistent contaminants, result of its high stability in the environment [6, 7].

An herbicide that has been extensively used since 1974 is glyphosate (*N*-(phosphfometila) glycine — $C_3H_8NO_5P$) (Fig. 1), which is an organophosphate with a broadly effective spectrum, non-selective, and being one of the most used herbicides in the world [6–8]. The solubility of glyphosate in water is 12 g L^{-1} [9] which justifies, together with its extensive use, its frequent detection in aquatic environments, especially groundwater from soils with shallow water table and/or low in oxides [6].

This paper belongs to the Topical Collection VIII Symposium on Electronic Structure and Molecular Dynamics – VIII SeedMol

✉ Douglas Henrique Pereira
doug@uft.edu.br

[1] Chemistry Collegiate, Federal University of Tocantins, Campus Gurupi - Badejós, P.O. Box 66, Gurupi, Tocantins 77 402-970, Brazil

[2] Federal Institute of Tocantins, Campus Dianópolis - Rodovia TO - 040 - Km 349, Lote 01 - Loteamento Rio Palmeiras, Dianópolis, Tocantins 77300-000, Brazil

[3] Institute of Chemistry, University of Campinas – UNICAMP, P.O. Box 6154, Campinas, São Paulo 13083-970, Brazil

Glyphosate can cause numerous environmental problems because it blocks an enzymatic pathway that exists only in plants and bacteria and has a toxic effect on animals [8, 10]. In this context, ways to remove this pollutant, mainly from water bodies, are of paramount importance for the protection of ecosystems and maintenance of biodiversity, requiring efficient methods with technological and economic feasibility of application [11]. Among the most used removal methods are adsorptive processes, which give good quality to the treated effluent, operational flexibility, possibility of adsorbent regeneration, and effective and economical method [12].

Activated charcoal, as adsorbent, is still widely used, removing dyes [13], metals [14, 15], and radionuclides [16], among other pollutants; however, it is a high-value alternative [8]. Thus, the search for low-cost adsorbents [11], such as agricultural waste [17, 18] and industrial by-products [19], and natural substances such as minerals [20, 21] and biopolymers [22, 23] have increased.

In the biopolymers class, cellulose stands out because it is abundant [24], presents good potential as adsorbent material, and is a non-toxic, hydrophilic, biodegradable, and chemically modifiable material [25–27]. Its application extends to some derivatives such as cellulose acetate, diethylaminoetil cellulose, cellulose xanthate, methylcellulose, and nitrocellulose among others that have applications in several areas besides adsorption [28–36].

Cellulose, together with some derivatives such as cellulose acetate, carboxymethylcellulose, and cellulose xanthate, were theoretically studied by Reis et al. [22, 37] using calculations based on the density functional theory (DFT). The biopolymers proved to be excellent adsorptive matrices for Cd^{2+}, Cu^{2+}, and Cr^{3+} metals, providing promising prospects for the application of cellulose and its derivatives.

In this context, in view of the gradual increase in glyphosate concentrations in the environment and the excellent adsorptive capacity of cellulose and derivatives, the present work aims to evaluate from theoretical calculations the interaction of glyphosate with cellulose and its diethylaminoethyl cellulose derivative in order to verify the potential for contaminant removal. It is worth mentioning that the need for efficient adsorptive materials for removing contaminants is urgent and many possibilities need to be evaluated, which makes theoretical studies the best alternatives for directing experimental research, optimizing study time, and contributing with relevant structural information on biopolymers and glyphosate.

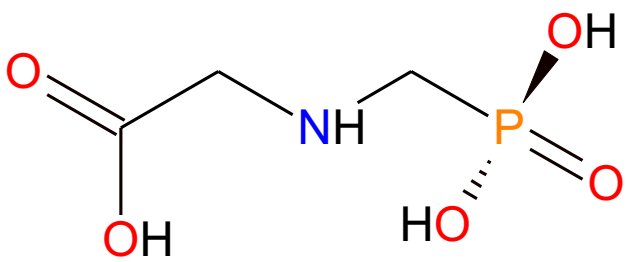

Fig. 1 Structural representation of the glyphosate molecule

Computational methods

The studies of adsorptive processes were carried out using the DFT [38–41] with the hybrid functional wB97XD [42] and basis set 6–31 + G(d,p) [43–45]. The structures of the adsorption matrices of cellulose (CE) and diethylaminoetil cellulose (DEAEC) and the glyphosate adsorbate (GLY) were optimized to the minimum of energy. To confirm that optimized structures were at their minimum energy, frequency calculations were used and no imaginary frequency was found. No dispersion model was included, because the functional wB97XD has empirical corrections of atom–atom dispersion ($E_{\text{DFT-D}} = E_{\text{KS-DFT}} - E_{\text{disp.}}$) [42, 46–48]. The effect of water as solvent was considered in the optimization and in all calculations using the continuous solvent model SMD [49]. The basis set superposition error (BSSE) was not used because in previous work, it was evaluated that the effect of the solvent significantly modifies the results of the interaction process [50] and the BSSE is evaluated for gas phase.

The energies of the molecular orbitals HOMO (highest occupied molecular orbital) and LUMO (lowest unoccupied molecular orbital) were used to obtain chemical hardness (η) and chemical softness (S). By DFT, chemical hardness can be calculated by Eq. 1 [51]:

$$\eta = \frac{1}{2}(E_{\text{LUMO}} - E_{\text{HOMO}}) \tag{1}$$

where $E_{\text{LUMO}} - E_{\text{HOMO}}$ are the energies of the LUMO and HOMO, respectively. Equation 1 can be used taking into account Koopmans' theorem [52].

Chemical softness is the inverse of hardness and was determined by Eq. 2:

$$S = \frac{1}{\eta} \tag{2}$$

Frontier molecular orbitals (FMOs) and molecular electrostatic maps (MEPs) were generated with isovalue 0.02 and density 0.001 au, respectively.

The binding energy (E_{Bind}) of the interaction process was quantified by Eq. 3:

$$E_{\text{bind}} = E_{\text{complex}} - [E_{\text{adsorbent}} + E_{\text{adsorbate}}] \tag{3}$$

where E_{complex} corresponds to the energy of the complex (adsorbent + adsorbate) and $E_{\text{adsorbent}}$ and $E_{\text{adsorbate}}$ are the electronic energies of the adsorbent (adsorptive matrix) and adsorbate (glyphosate), respectively. In the electronic energy

was added the zero point energy (ZPE). The Gibbs energy (ΔG) and enthalpy (ΔH) were also determined by the difference of the energies (Gibbs and enthalpy) of complex subtracted from the isolated values of the molecules, Eqs. 4 and 5:

$$\Delta G = G_{\text{complex}} - [G_{\text{adsorbent}} + E_{\text{adsorbate}}] \quad (4)$$

$$\Delta H = H_{\text{complex}} - [H_{\text{adsorbent}} + H_{\text{adsorbate}}] \quad (5)$$

All calculations were performed using the Gaussian 09 program [53] and some structures were drawn with the Gauss View program [54].

To characterize the interactions between glyphosate and biopolymers, as well as the nature of the interaction, QTAIM analyses [55–59] were performed. The parameters considered in the analyzes were electronic density ($\rho(r)$), laplacian of electronic density ($\nabla^2\rho(r)$), potential energy density ($V(r)$), kinetic energy density ($G(r)$), and energy density at the bond critical point (BCP) ($H(r)$), used for all complexes. The laplacian of electronic density allows analyzing the nature of the bond/interaction. $\nabla^2\rho(r) < 0$ refers to a covalent bond, while $\nabla^2\rho(r) > 0$ indicates noncovalent bond. A joint analysis with the energy density in BCP ($H(r) = G(r) + V(r)$) allows a more detailed description, in which $\nabla^2\rho(r) > 0$ and $H(r) > 0$ indicates that the bond, or interaction, will be electrostatic, while $\nabla^2\rho(r) > 0$ and $H(r) < 0$ indicate that the interaction is partially covalent. All QTAIM analyses were performed using the AIMALL package [60].

Results and discussion

Structures before complexation

The biopolymers CE and DEAEC were studied using three monomeric units of each and the cut ends were completed with hydrogen atoms. This methodology was previously used by the research group [22, 23, 37] in order to achieve a lower computational cost and reduce as much as possible the loss of the original properties of CE and DEAEC. In addition to the CE, the study of the DEAEC was motivated by studies in the literature, which suggest that modified cellulose, that is, with different functional groups inserted in its structure, lead to a higher adsorption potential.

To reproduce the possibilities of adsorption of the experimental data, two oxygen were deprotonated from CE and DEAEC. In this context, the DEAEC and CE present regions with negative charges and the DEAEC presents electropositive regions, which allow evaluating the adsorption potential of biopolymers under these conditions [50, 61–63]. Only the adsorptive matrices were modified and the adsorbate (glyphosate) was kept in its neutral form.

Initially, an analysis of possible sites of interaction was performed and the analysis of molecular electrostatic potential (MEP), FMOs, and reactivity indices (RI) was used.

The molecular structures MEPs and FMOs for CE and DEAEC biopolymers are represented in Fig. 2. For MEPs, colors in blue tones indicate partially positive regions while red/orange colors are partially negative regions. MEP values are also represented in kcal mol^{-1} (Fig. 2). Thus, it is found that for CE, the MEP shows that the regions with the highest negative partial charges are concentrated in the region of ($-O^-$) with values of $\cong -225.90$ kcal mol^{-1} and -213.35 kcal mol^{-1}. The DEAEC presents higher negative partial charges in the anionic oxygen groups ($-O^-$) ($\cong -163.15$ kcal mol^{-1}); on the other side of the DEAEC structure, it is possible to observe a positive partial charge region located in the protonated amine group ($-NH^+(CH_2CH_3)_2$), $\cong 89.98$ kcal mol^{-1}.

Analyzing the FMOs (Fig. 2), the HOMO and LUMO of the CE and DEAEC matrices can be observed. For CE, a LUMO with probability density is observed in groups –OH, while the HOMO have π orbitals in the anionic oxygen group $-O^-$.

The DEAEC biopolymer has a high probability density in the group $-NH^+(CH_2CH_3)_2$ for LUMO and, at the left end, regions with some probability density for the HOMO.

Figure 3 shows the MEP and the FMOs for adsorbate. It can be observed that GLY presents a LUMO orbital with a high probability density (Fig. 3a), which indicates that an interaction may occur between LUMO (adsorbate) and HOMO orbitals of the adsorbent. On the other hand, the HOMO shows possibilities of interaction with $-O^-$ group, nitrogen and hydrogen along the molecule chain.

Analyzing the MEP for the GLY (Fig. 3b), one can observe predominantly green and blue regions, that is, GLY has positive partial charges in most of its structure (values of MEPs $\cong 25.10$ kcal mol^{-1}, 59.55 kcal mol^{-1}, and 31.38 kcal mol^{-1}). A reddish region can be observed in the oxygen atom of the phosphate group ($-PO(OH)_2$), $\cong -45.81$ kcal mol^{-1}, indicating that the molecule has a significant negative partial charge in this structural part.

From the energy of the HOMO and LUMO orbitals, the reactivity indices hardness (η) and softness (S) were determined (Table 1) and follows Pearson's acid–base theory [64, 65].

The results of Table 1 show that the chemical softness and hardness are similar and it is possible to suggest that the interaction of GLY with both CE and DEAEC will be effective due to the proximity of the reactivity indices as expressed by Pearson's concept [64, 65].

Analyzing in a general way the results of the FMO, MEP, and RI, it is possible to infer the importance of the quantum descriptors for the adsorption process because they allow

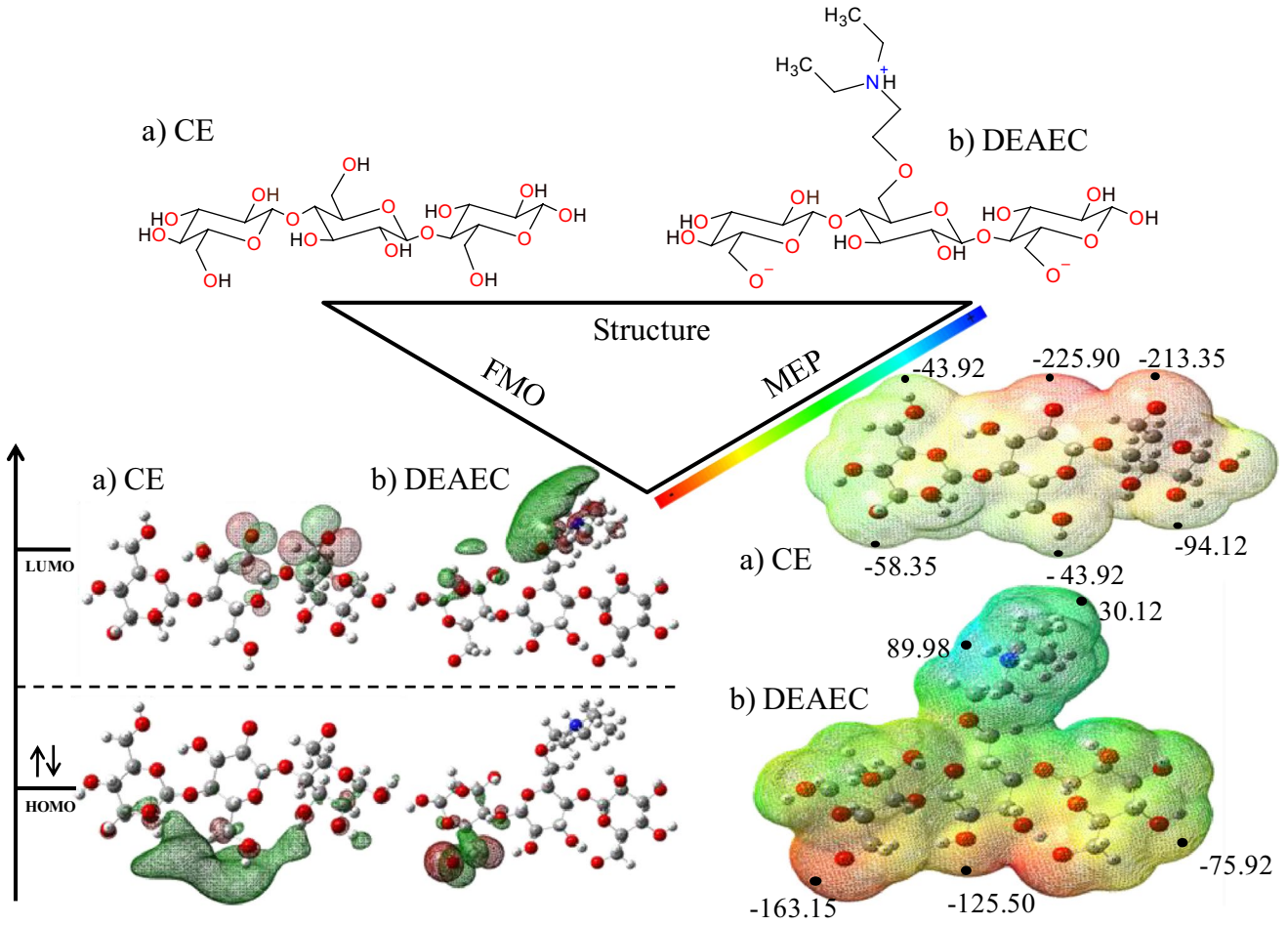

Fig. 2 Structural formula, molecular electrostatic potential and frontier molecular orbitals (HOMO and LUMO) for **a** cellulose and **b** diethylaminoethyl cellulose. Values of MEPs in kcal mol^{-1}

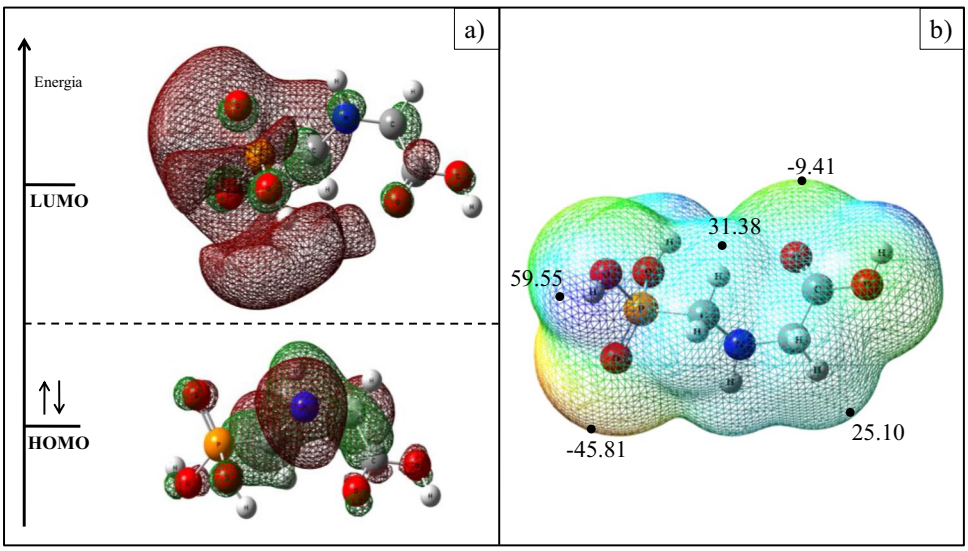

Fig. 3 Representation of the frontier molecular orbitals LUMO and HOMO in (**a**) and in (**b**) molecular electrostatic potential of glyphosate. Values of the MEP in kcal mol^{-1}

Table 1 Values of HOMO, LUMO, hardness (η), and softness (S) for the matrices (adsorbents) and the contaminant (adsorbate). Data in kcal mol^{-1}

	HOMO	LUMO	(η)	(S)
GLY	− 207.89	35.479	121.69	0.0082
CE	− 174.61	43.173	108.89	0.0092
DEAEC	− 177.48	42.225	109.85	0.0091

to predict the interaction site, if the matrices will interact properly with the contaminate, reducing computational time, and are able to assist in the experimental part as described in several works [21, 66].

Complex structures

The post-complexation analyses were performed using the results obtained from the analyses of FMOs, MEPs, and reactivity index. The sites chosen to adsorb GLY in biopolymers were terminal groups $–O^-$ and –OH for CE and for DEAEC in the $–O^-$ and $–NH^+(CH_2CH_3)_2$ groups. The study was carried out using optimized structures. Figures 4 and 5 show the interaction sites analyzed.

The vibrational frequencies and the interaction bond lengths of the complexes formed were determined and are represented in Table 2. The bond distances determined ranged from 1.68 to 3.11 Å, indicating that the interaction actually occurs due to the proximity of the molecules. It is important to emphasize that the interactions are formed predominantly by hydrogen bonds (Figs. 4 and 5) and that the interactions of GLY with CE were those with lower bond lengths when compared to interactions in DEAEC.

Experimental infrared (IR) data for glyphosate [68–72] show that the vibrational band between 1600 and 1800 cm^{-1} is attributed to the $–CO_2$ group (C = O). The PO_3H_2 group showed stretching bands at 911–1223 cm^{-1} attributed to P-OH and bands in the region of 1090–1094 cm^{-1} and 1268–1271 cm^{-1} corresponding to $P\text{-}O^-$ and P = O, respectively. Angular deformations in the region of 830 cm^{-1} (P–O–H) and between 1483 and 1563 cm^{-1} correspond to

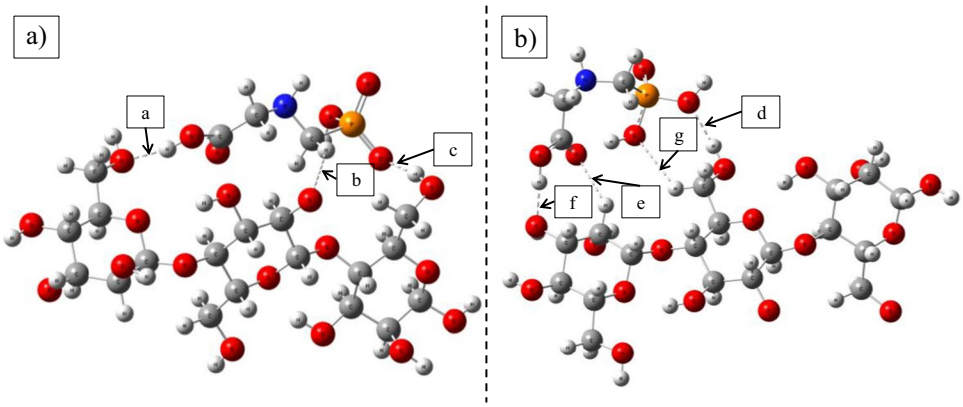

Fig. 4 Spatial arrangement and interaction positions for GLY and CE. In **a** configuration 01 (CE-GLY^1) and in **b** configuration 02 (CE-GLY^2)

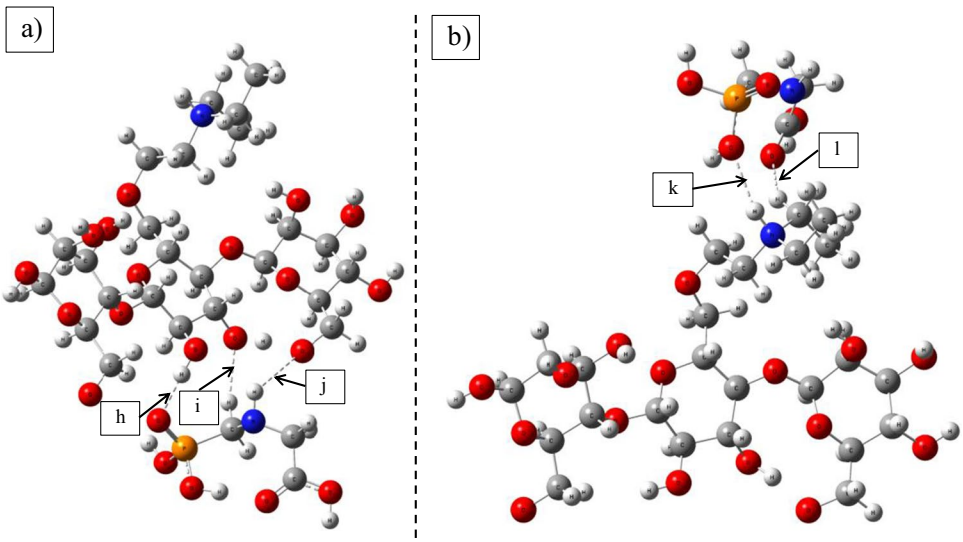

Fig. 5 Spatial arrangement and interaction positions for GLY and DEAEC. In **a** configuration 01 (DEAEC-GLY^1) and **b** configuration 02 (DEAEC-GLY^2)

Table 2 Calculated interaction distances (in Å) and vibrational frequencies (in cm^{-1}) of GLY, CE, DEAEC, and complexes formed

Adsorbate/adsorbent/complex	Interaction position	Interaction distance	Type/frequency
GLY	d,g,k	-	δ(P–O–H)/874.23
	c,h	-	ν(P=O)/1218.56
	j	-	δ(C–N–H)/1508.51
	e	-	ν(C=O)/1777.17
CE	a	-	ν(C–O)/1106.41
	b	-	ν(C–O)/1135.97
	c	-	ν(C–O)/1240.50
	d	-	ν(C–O)/1084.84
	e	-	ν(C–O)/1199.74
	f	-	ν(C–O)/1151.81
	g	-	ν(C–H)/3060.93
DEAEC	h	-	ν(C–O)/1208.34
	i	-	ν(C–O)/1163.63
	j	-	ν(C–O)/1066.99
	k	-	ν(N–H)/3490.87
	l	-	ν(C–H)/3213.32
CE-GLY[1]	a	1.68	ν(C–O)/1059.22
	b	2.86	ν(C–O)/ 1137.32
	c	1.74	ν(C–O)/ 1149.84
			ν(P=O)/1196.50
CE-GLY[2]	d	1.89	ν(C–O)/1107.78
			δ(P–O–H)/872.51
	e	2.57	ν(C=O)/1724.34
	f	1.65	ν(C–O)/1112.60
	g	2.97	ν(C–H)/3022.25
			δ(P–O–H)/888.02
DEAEC-GLY[1]	h	1.79	ν(C–O)/1224.91
			ν(P=O)/1195.48
	i	2.26	ν(C–O)/1191.51
	j	3.11	ν(C–O)/1115.96
			δ(C-N–H)/1473.15
DEAEC-GLY[2]	k	2.18	ν(N–H)/3459.64
			δ(P–O–H)/867.53
	l	2.42	ν(C–H)/3216.09

C–N–H. According to the literature, these are characteristic bands for glyphosate at pH = 7 [67–71]. The theoretical results for glyphosate are close or within the experimental ranges (Table 2) proving that the calculations adequately describe the GLY molecule. The experimental IV for CE and DEAEC were not reported in the present work because only three monomeric units of each polymer were considered theoretically and the results may not be as suitable as for GLY.

Simulated IR after complexation showed that there is a change in vibrational bands for GLY and for the matrices (Table 2) and can be evidenced in experimental measurements proving the interaction.

Table 3 The binding energy (E_{Bind}) at 0 K, enthalpy (ΔH), and Gibbs energy (ΔG) at 298 K for the complexes studied. Values in kcal mol^{-1}

Complex	E_{Bind}	ΔH	ΔG
CE-GLY[1]	−45.11	−45.70	−27.30
CE-GLY[2]	−14.50	−15.03	1.52
DEAEC-GLY[1]	−11.39	−11.81	1.52
DEAEC-GLY[2]	−8.18	−7.02	4.50

Adsorption processes involve the interaction of atoms, ions, or molecules with a surface and this interaction is due to energies derived from the electronic stability of each chemical species involved in the adsorption process. In this sense, the binding energy (E_{Bind}), Gibbs energy (ΔG), and enthalpy (ΔH) involved in the interactions were calculated and are represented in Table 3. The energies were obtained in order to observe the magnitude of the interactions of the complexes formed and the spontaneity related to each interaction.

From the results shown in Table 3, it can be noted that for E_{Bind} in general, the CE and DEAEC are good adsorption matrices for removing the GLY contaminant. The interaction of GLY with the biopolymers CE and DEAEC in configuration 01 were those that presented values E_{Bind} most significant for the adsorption process, which indicates that the interaction sites of Figs. 4a and 5a are the ones that best interact with the GLY molecule sites. The bond lengths for the complexes in configuration 01 were also the smallest as noted in Table 2.

The negative values ΔH prove that all processes are exothermic. The CE-GLY[1] interaction showed value of $\Delta G < 0$ indicating that this interaction is spontaneous ($\Delta G = -27.30$ kcal mol^{-1}). It is noteworthy that the effect of the solvent significantly alters the Gibbs energy values of the adsorption process as highlighted by Costa et al. [50].

In order to characterize the nature of the interactions for the complexes formed, the topological analysis QTAIM was performed and the results are shown in Table 4. Table 4 presents all topological parameters obtained from Quantum Theory of Atoms in Molecules by Bader et al. [56–58] for the interactions found (Figs. 4 and 5).

From the topological parameters, there are the following considerations: the electronic density can give indications of the strength of the interaction indirectly, because a higher value of electronic density is related to a greater bond force in the interaction BCP [71]. The CE-GLY[1] complex has two strongest interactions *a* and *c* with values of $\rho(r) = 0.046006$ u.a. and $\rho(r) = 0.038594$ u.a. and the CE-GLY[2] has only one strongest interaction *f* with value of $\rho(r) = 0.049337$ u.a. DEAEC-GLY[1] has one strong interaction *h* ($\rho(r) = 0.034768$

Table 4 Topological parameters calculated in the BCPs of the interactions. Values in atomic units (au)

Complex	Interaction (BCP)	$\rho(r)$	$\nabla^2\rho(r)$	$V(r)$	$G(r)$	$H(r)$
CE-GLY[1]	a (O_{16}-H_{71})	0.046006	+0.133216	−0.035150	+0.034227	−0.000923
	b (O_{33}-H_{75})	0.005916	+0.018153	−0.003184	+0.003861	+0.000677
	c (O_{80}-H_{81})	0.038594	+0.120323	−0.029487	+0.029784	+0.000297
CE-GLY[2]	d (O_{80}-H_{40})	0.026733	+0.082789	−0.020437	+0.020567	+0.000130
	e (O_{69}-H_{43})	0.008373	+0.029104	−0.005530	+0.006403	+0.000873
	f (O_{11}-H_{71})	0.049337	+0.140419	−0.038560	+0.036832	−0.001728
	g (O_{78}-H_{38})	0.003715	+0.014555	−0.002030	+0.002834	+0.000804
DEAEC-GLY[1]	h (H_{33}-O_{103})	0.034768	+0.106464	−0.026408	+0.026512	+0.000104
	i (O_{30}-H_{96})	0.015842	+0.043943	−0.011613	+0.011299	−0.000313
	j (O_{16}-H_{94})	0.007710	+0.028417	−0.005466	+0.006285	+0.000819
DEAEC-GLY[2]	k (H_{55}-O_{99})	0.014307	+0.047791	−0.011304	+0.011626	+0.000322
	l (H_{54}-O_{90})	0.009942	+0.033793	−0.007005	+0.007726	+0.000722

u.a) and for DEAEC-GLY[2], the interaction *k* is the most significant ($\rho(r) = 0.014307$ u.a.). The $\rho(r)$ values reflect the proximity of the contaminate with the matrices as described by the bond lengths of the interactions (Table 2).

The laplacians of electronic density are positive, indicating non-covalent interaction. The interactions *a*, *f*, and *i* are partially covalent according to the values of $\nabla^2\rho(r)$ and $H(r)$. All other interactions found are electrostatic interactions, which adequately reflect the energy values found.

The interaction energies in the BCPs can also be estimated by the relation $E_{int} = V(r)/2$ [62, 72]. From the results (Table 4), it is possible to infer that the most effective interactions are *a* and *c* for CE-GLY[1]; *f* for CE-GLY[2]. For DEAEC-GLY[1] is the interactions *h* and DEAEC-GLY[2] is the interaction *k*. E_{int} values reflect the trend found for E_{Bind} and the bond lengths of the interactions.

Conclusion

The study presented the results obtained from the interactions of the cellulose and diethylaminoethyl cellulose matrices with the herbicide glyphosate, in order to verify the potential for removal of the contaminant. The analysis of MEPs, FMOs, and reactivity indices allowed to infer the probable sites of interaction of the matrices with the herbicide that were in the groups $–O^-$ and –OH of cellulose and in the groups $–O^-$ and $–NH^+(CH_2CH_3)_2$ of DEAEC. The QTAIM analysis corroborated with the results obtained for binding energy. Thus, the use of cellulose and diethylaminoethyl cellulose biopolymers as adsorption matrices for the removal of the glyphosate herbicide from water bodies is feasible from a theoretical point of view, presenting good results that, theoretically, enable its use as an adsorbent material for removing the herbicide.

Author contribution Sílvio Quintino de Aguiar Filho: Conceptualization, Methodology, Validation, Formal analysis. Adão Marcos Ferreira Costa: Visualization, Software, Formal analysis. Anna Karla dos Santos Pereira: Writing — review and editing, Visualization, Software. Grasiele Soares Cavallini: Writing — original draft, Writing — review and editing, Conceptualization, Methodology. Douglas Henrique Pereira: Writing — original draft, Writing — review and editing, Conceptualization, Methodology, Formal analysis.

Funding The authors acknowledge funding from CAPES (Coordination of Improvement of Higher Education Personnel, Brazil, Funding Code 001 CAPES) and the PROPESQ/Federal University of Tocantins (Edital para tradução de artigos científicos da Universidade Federal do Tocantins, PROPESQ/UFT). The Center for Computational Engineering and Sciences (financial support from FAPESP Fundação de Amparo à Pesquisa, Grant 2013/08293–7 and Grant 2017/11485–6) and the National Center for High Performance Processing (Centro Nacional de Processamento de Alto Desempenho – CENAPAD) in São Paulo for computational resources.

Availability of data and material Not applicable.

Code availability Not applicable.

Declarations

Ethics approval and consent to participate Not applicable.

Consent for publication Not applicable.

Competing interests The authors declare no competing interests.

References

1. Nakka S, Jugulam M, Peterson D, Asif M (2019) Herbicide resistance: development of wheat production systems and current status of resistant weeds in wheat cropping systems. The Crop Journal, Breeding wheat for the global north: China, the USA and Canada 7:750–760. https://doi.org/10.1016/j.cj.2019.09.004
2. Oerke E-C (2006) Crop losses to pests. J Agric Sci 144:31–43. https://doi.org/10.1017/S0021859605005708

3. Croll BT (1991) Pesticides in surface waters and groundwaters. Water and Environment Journal 5:389–395. https://doi.org/10.1111/j.1747-6593.1991.tb00635.x
4. Ollinger M, Aspelin A, Shields M (1998) US regulation and new pesticide registrations and sales. Agribusiness 14:199–212. https://doi.org/10.1002/(SICI)1520-6297(199805/06)14:3%3c199::AID-AGR3%3e3.0.CO;2-W
5. Pelaez V, da Silva LR, Araújo EB (2013) Regulation of pesticides: a comparative analysis. Sci Public Policy 40:644–656. https://doi.org/10.1093/scipol/sct020
6. Ramrakhiani L, Ghosh S, Mandal A, Majumdar S (2019) Utilization of multi-metal laden spent biosorbent for removal of glyphosate herbicide from aqueous solution and its mechanism elucidation. Chem Eng J 361:1063–1077. https://doi.org/10.1016/j.cej.2018.12.163
7. Fiorilli S, Rivoira L, Calì G, Appendini M, Bruzzoniti MC, Coïsson M, Onida B (2017) Iron oxide inside SBA-15 modified with amino groups as reusable adsorbent for highly efficient removal of glyphosate from water. Appl Surf Sci 411:457–465. https://doi.org/10.1016/j.apsusc.2017.03.206
8. Feng D, Malleret L, Soric A, Boutin O (2020) Kinetic study of glyphosate degradation in wet air oxidation conditions. Chemosphere 247:125930. https://doi.org/10.1016/j.chemosphere.2020.125930
9. Gros P, Ahmed A, Kühn O, Leinweber P (2017) Glyphosate binding in soil as revealed by sorption experiments and quantum-chemical modeling. Sci Total Environ 586:527–535. https://doi.org/10.1016/j.scitotenv.2017.02.007
10. World Health Organization (WHO) (2016). World https://www.who.int/foodsafety/jmprsummary2016.pdf?ua=1. Accessed 19 Jul 2021
11. Castiglioni S, Bagnati R, Fanelli R, Pomati F, Calamari D, Zuccato E (2006) Removal of pharmaceuticals in sewage treatment plants in Italy. Environ Sci Technol 40:357–363. https://doi.org/10.1021/es050991m
12. Fu F, Wang Q (2011) Removal of heavy metal ions from wastewaters: a review. J Environ Manage 92:407–418. https://doi.org/10.1016/j.jenvman.2010.11.011
13. Crini G, Lichtfouse E, Wilson LD, Morin-Crini N (2019) Conventional and non-conventional adsorbents for wastewater treatment. Environ Chem Lett 17:195–213. https://doi.org/10.1007/s10311-018-0786-8
14. Babel S, Kurniawan TA (2003) Low-cost adsorbents for heavy metals uptake from contaminated water: a review. J Hazard Mater 97:219–243. https://doi.org/10.1016/S0304-3894(02)00263-7
15 Ince M, Kaplan Ince O (2017) An overview of adsorption technique for heavy metal removal from water/wastewater: a critical review. International Journal of Pure and Applied Sciences 3:10–19. https://doi.org/10.29132/ijpas.358199
16. Abu-Dalo MA, Nevostrueva S, Hernandez M (2020) Removal of radionuclides from acidic solution by activated carbon impregnated with methyl- and carboxy-benzotriazoles. Sci Rep 10:11712. https://doi.org/10.1038/s41598-020-68645-4
17. Hameed BH, Krishni RR, Sata SA (2009) A novel agricultural waste adsorbent for the removal of cationic dye from aqueous solutions. J Hazard Mater 162:305–311. https://doi.org/10.1016/j.jhazmat.2008.05.036
18. Dai Y, Sun Q, Wang W, Lu L, Liu M, Li J, Yang S, Sun Y, Zhang K, Xu J, Zheng W, Hu Z, Yang Y, Gao Y, Chen Y, Zhang X, Gao F, Zhang Y (2018) Utilizations of agricultural waste as adsorbent for the removal of contaminants: a review. Chemosphere 211:235–253. https://doi.org/10.1016/j.chemosphere.2018.06.179
19. Geethakarthi A, Phanikumar BR (2010) Industrial sludge based adsorbents/industrial by-products in the removal of reactive dyes A review. IJWREE 3:1–9. https://doi.org/10.5897/IJWREE.9000029
20. Wang S, Peng Y (2010) Natural zeolites as effective adsorbents in water and wastewater treatment. Chem Eng J 156:11–24. https://doi.org/10.1016/j.cej.2009.10.029
21. Resende RF, Leal PVB, Pereira DH, Papini RM, Magriotis ZM (2020) Removal of fatty acid by natural and modified bentonites: elucidation of adsorption mechanism. Colloids Surf, A 605:125340. https://doi.org/10.1016/j.colsurfa.2020.125340
22. Reis DT, Ribeiro IHS, Pereira DH (2020) DFT study of the application of polymers cellulose and cellulose acetate for adsorption of metal ions (Cd2+, Cu2+ and Cr3+) potentially toxic. Polym Bull 77:3443–3456. https://doi.org/10.1007/s00289-019-02926-5
23. Ribeiro IHS, Reis DT, Pereira DH (2019) A DFT-based analysis of adsorption of Cd2+, Cr3+, Cu2+, Hg2+, Pb2+, and Zn2+, on vanillin monomer: a study of the removal of metal ions from effluents. J Mol Model 25:267. https://doi.org/10.1007/s00894-019-4151-z
24 O'Connell DW, Birkinshaw C, O'Dwyer TF (2008) Heavy metal adsorbents prepared from the modification of cellulose: a review. Bioresource Technology 99:6709–6724. https://doi.org/10.1016/j.biortech.2008.01.036
25. Suhas Gupta VK, Carrott PJM, Singh R, Chaudhary M, Kushwaha S (2016) Cellulose: a review as natural, modified and activated carbon adsorbent. Biores Technol 216:1066–1076. https://doi.org/10.1016/j.biortech.2016.05.106
26. Rahman NSA, Yhaya MF, Azahari B, Ismail WR (2018) Utilisation of natural cellulose fibres in wastewater treatment. Cellulose 25:4887–4903. https://doi.org/10.1007/s10570-018-1935-8
27. Varghese AG, Paul SA, Latha MS (2019) Remediation of heavy metals and dyes from wastewater using cellulose-based adsorbents. Environ Chem Lett 17:867–877. https://doi.org/10.1007/s10311-018-00843-z
28. Fischer S, Thümmler K, Volkert B, Hettrich K, Schmidt I, Fischer K (2008) Properties and applications of cellulose acetate. Macromol Symp 262:89–96. https://doi.org/10.1002/masy.200850210
29. Yang XH, Zhu WL (2007) Viscosity properties of sodium carboxymethylcellulose solutions. Cellulose 14:409–417. https://doi.org/10.1007/s10570-007-9137-9
30. Morozova S (2020) Methylcellulose fibrils: a mini review. Polym Int 69:125–130. https://doi.org/10.1002/pi.5945
31. Pourmortazavi SM, Hosseini SG, Rahimi-Nasrabadi M, Hajimirsadeghi SS, Momenian H (2009) Effect of nitrate content on thermal decomposition of nitrocellulose. J Hazard Mater 162:1141–1144. https://doi.org/10.1016/j.jhazmat.2008.05.161
32. Menefee E, Hautala E (1978) Soil stabilisation by cellulose xanthate. Nature 275:530–532. https://doi.org/10.1038/275530a0
33. Beyki MH, Bayat M, Miri S, Shemirani F, Alijani H (2014) Synthesis, characterization, and silver adsorption property of magnetic cellulose xanthate from acidic solution: prepared by one step and biogenic approach. Ind Eng Chem Res 53:14904–14912. https://doi.org/10.1021/ie501989q
34. Frank RA, Kavanagh R, Burnison BK, Headley JV, Peru KM, Der Kraak GV, Solomon KR (2006) Diethylaminoethyl-cellulose clean-up of a large volume naphthenic acid extract. Chemosphere 64:1346–1352. https://doi.org/10.1016/j.chemosphere.2005.12.035
35. Heri W, Neukom H, Deuel H (1961) Chromatographische Fraktionierung von Pektinstoffen an Diäthylaminoäthyl-Cellulose. 15. Mitteilung über Ionenaustauscher Helvetica Chimica Acta 44:1939–1945. https://doi.org/10.1002/hlca.19610440715
36. Smit CJB, Bryant EF (1967) Properties of pectin fractions separated on diethylaminoethyl-cellulose Columns. J Food Science 32:197–199. https://doi.org/10.1111/j.1365-2621.1967.tb01292.x
37. Reis DT, de Aguiar Filho SQ, Grotto CGL, Bihain MFR, Pereira DH (2020) Carboxymethylcellulose and cellulose xanthate matrices as potential adsorbent material for potentially toxic Cr3+,

Cu2+ and Cd2+metal ions: a theoretical study. Theor Chem Acc 139:96. https://doi.org/10.1007/s00214-020-02610-2
38. Hohenberg P, Kohn W (1964) Inhomogeneous electron gas. Phys Rev 136:B864–B871. https://doi.org/10.1103/PhysRev.136.B864
39. Kohn W, Sham LJ (1965) Self-consistent equations including exchange and correlation effects. Phys Rev 140:A1133–A1138. https://doi.org/10.1103/PhysRev.140.A1133
40. Parr RG (1989) W. Yang Density functional theory of atoms and molecules. Oxford University Press 1, 1989
41. Becke AD (2014) Perspective: fifty years of density-functional theory in chemical physics. J Chem Phys 140:18A301. https://doi.org/10.1063/1.4869598
42. Chai J-D, Head-Gordon M (2008) Long-range corrected hybrid density functionals with damped atom–atom dispersion corrections. Phys Chem Chem Phys 10:6615–6620. https://doi.org/10.1039/B810189B
43. Ditchfield R, Hehre WJ, Pople JA (1971) Self-consistent molecular-orbital methods. IX. An extended Gaussian-type basis for molecular-orbital studies of organic molecules. J Chem Phys 54:724–728. https://doi.org/10.1063/1.1674902
44. Hehre WJ, Ditchfield R, Pople JA (1972) Self-consistent molecular orbital methods. XII. Further extensions of Gaussian-type basis sets for use in molecular orbital studies of organic molecules. J Chem Phys 56:2257–2261. https://doi.org/10.1063/1.1677527
45. Hariharan PC, Pople JA (1973) The influence of polarization functions on molecular orbital hydrogenation energies. Theoret Chim Acta 28:213–222. https://doi.org/10.1007/BF00533485
46. Liu Y, Liu Y, Gallo AA, Knierim KD, Taylor ER, Tzeng N (2015) Performances of DFT methods implemented in G09 for simulations of the dispersion-dominated CH-π in ligand–protein complex: a case study with glycerol-GDH. J Mol Struct 1084:223–228. https://doi.org/10.1016/j.molstruc.2014.12.028
47. Matczak P (2015) Assessment of various density functionals for intermolecular N→Sn interactions: the test case of poly(trimethyltin cyanide). Comput Theor Chem 1051:110–122. https://doi.org/10.1016/j.comptc.2014.10.028
48. Rayne S, Forest K (2016) A comparative examination of density functional performance against the ISOL24/11 isomerization energy benchmark. Comput Theor Chem 1090:147–152. https://doi.org/10.1016/j.comptc.2016.06.018
49. Marenich AV, Cramer CJ, Truhlar DG (2009) Universal solvation model based on solute electron density and on a continuum model of the solvent defined by the bulk dielectric constant and atomic surface tensions. J Phys Chem B 113:6378–6396. https://doi.org/10.1021/jp810292n
50. Costa AMF, de Aguiar Filho SQ, Santos TJ, Pereira DH (2021) Theoretical insights about the possibility of removing Pb2+ and Hg2+ metal ions using adsorptive processes and matrices of carboxymethyldiethylaminoethyl cellulose and cellulose nitrate biopolymers. J Mol Liq 331:115730. https://doi.org/10.1016/j.molliq.2021.115730
51. Parr RG, Donnelly RA, Levy M, Palke WE (1978) Electronegativity: the density functional viewpoint. J Chem Phys 68:3801–3807. https://doi.org/10.1063/1.436185
52. Koopmans T (1934) Über die Zuordnung von Wellenfunktionen und Eigenwerten zu den Einzelnen Elektronen Eines Atoms. Physica 1:104–113. https://doi.org/10.1016/S0031-8914(34)90011-2
53. Frisch MJ, Trucks GW, Schlegel HB, Scuseria GE, Robb MA, Cheeseman JR, Scalmani G, Barone V, Mennucci B, Petersson GA, Nakatsuji H, Caricato M, Li X, Hratchian HP, Izmaylov AF, Bloino J, Zheng G, Sonnenberg JL, Hada M, Ehara M, Toyota K, Fukuda R, Hasegawa J, Ishida M, Nakajima T, Honda Y, Kitao O, Nakai H, Vreven T, Montgomery JA, Peralta JE Jr, Ogliaro F, Bearpark M, Heyd JJ, Brothers E, Kudin KN, Staroverov VN, Kobayashi R, Normand J, Raghavachari K, Rendell A, Burant JC, Iyengar SS, Tomasi J, Cossi M, Rega N, Millam JM, Klene M, Knox JE, Cross JB, Bakken V, Adamo C, Jaramillo J, Gomperts R, Stratmann RE, Yazyev O, Austin AJ, Cammi R, Pomelli C, Ochterski JW, Martin RL, Morokuma K, Zakrzewski VG, Voth GA, Salvador P, Dannenberg JJ, Dapprich S, Daniels AD, Farkas Ö, Foresman JB, Ortiz JV, Cioslowski J, Fox DJ (2009) Gaussian 09, Revision D01, Gaussian, Inc., Wallingford, CT, 2009
54. Dennington R, Keith T, Millam JG (2009) Gauss View, Version 5. Semichem Inc., Shawnee Mission
55. Bader RFW, Essén H (1984) The characterization of atomic interactions. J Chem Phys 80:1943–1960. https://doi.org/10.1063/1.446956
56. Bader RFW (1990) Atoms in molecules: a quantum theory, 1st edn. Oxford Univ. Press, Oxford
57. Keith TA, Bader RFW, Aray Y (1996) Structural homeomorphism between the electron density and the virial field. Int J Quantum Chem 57:183–198. https://doi.org/10.1002/(SICI)1097-461X(1996)57:2%3c183::AID-QUA4%3e3.0.CO;2-U
58. Popelier PLA (1999) Quantum molecular similarity. 1. BCP Space J Phys Chem A 103:2883–2890. https://doi.org/10.1021/jp984735q
59. Kumar PSV, Raghavendra V, Subramanian V (2016) Bader's theory of atoms in molecules (AIM) and its applications to chemical bonding. J Chem Sci 128:1527–1536. https://doi.org/10.1007/s12039-016-1172-3
60. Todd A, Keith T (2017) AIMAll (Version 10.05. 04). Gristmill Software, Overland Park KS, USA.
61. Yakout AA, El-Sokkary RH, Shreadah MA, Abdel Hamid OG (2016) Removal of Cd(II) and Pb(II) from wastewater by using triethylenetetramine functionalized grafted cellulose acetate-manganese dioxide composite. Carbohyd Polym 148:406–414. https://doi.org/10.1016/j.carbpol.2016.04.038
62. Kenawy IM, Hafez MAH, Ismail MA, Hashem MA (2018) Adsorption of Cu(II), Cd(II), Hg(II), Pb(II) and Zn(II) from aqueous single metal solutions by guanyl-modified cellulose. Int J Biol Macromol 107:1538–1549. https://doi.org/10.1016/j.ijbiomac.2017.10.017
63. Khademian E, Salehi E, Sanaeepur H, Galiano F, Figoli A (2020) A systematic review on carbohydrate biopolymers for adsorptive remediation of copper ions from aqueous environments-part A: classification and modification strategies. Sci Total Environ 738:139829. https://doi.org/10.1016/j.scitotenv.2020.139829
64. Pearson RG (1968) Hard and soft acids and bases, HSAB, part 1: fundamental principles. J Chem Educ 45:581. https://doi.org/10.1021/ed045p581
65. Pearson RG (1968) Hard and soft acids and bases, HSAB, part II: underlying theories. J Chem Educ 45:643. https://doi.org/10.1021/ed045p643
66. Leal PVB, Pereira DH, Papini RM, Magriotis ZM (2021) Effect of dimethyl sulfoxide intercalation into kaolinite on etheramine adsorption: experimental and theoretical investigation. J Environ Chem Eng 9:105503. https://doi.org/10.1016/j.jece.2021.105503
67. Undabeytia T, Morillo E, Maqueda C (2002) FTIR study of glyphosate−copper complexes. J Agric Food Chem 50:1918–1921. https://doi.org/10.1021/jf010988w
68. Piccolo A, Celano G (1993) Modification of infrared spectra of the herbicide glyphosate induced by pH variation. J of Env Sc & Hlth, Part B 28:447–457. https://doi.org/10.1080/03601239309372835
69. de Santana H, Toni LRM, de BenetoliB LO et al (2006) Effect in glyphosate adsorption on clays and soils heated and characterization by FT–IR spectroscopy. Geoderma 136:738–750. https://doi.org/10.1016/j.geoderma.2006.05.012
70. Subramaniam V, Hoggard PE (1988) Metal complexes of glyphosate. J Agric Food Chem 36:1326–1329. https://doi.org/10.1021/jf00084a050

71. Miano TM, Piccolo A, Celano G, Senesi N (1992) Infrared and fluorescence spectroscopy of glyphosate-humic acid complexes. Sci Total Environ 123–124:83–92. https://doi.org/10.1016/0048-9697(92)90135-F
72. Soliman SM, Barakat A, Islam MS, Ghabbour HA (2018) Synthesis, crystal structure and DFT studies of a new dinuclear Ag(I)-malonamide complex. Molecules 23:888. https://doi.org/10.3390/molecules23040888